

Tumor Classification using Automatic Multi-Thresholding

Li-Hong Juang^a and Ming-Ni Wu^b

^aSchool of Electrical Engineering and Automation, Xiamen University of Technology, No.600, Ligong Road, Jimei, Xiamen, 360124, P.R.China; ^bDepartment of Information Management, National Taichung University of Technology, Taichung, Taiwan ROC

ABSTRACT

In this paper we explore these math approaches for medical image applications. The application of the proposed method for detection tumor will be able to distinguish exactly tumor size and region. In this research, some major design and experimental results of tumor objects detection method for medical brain images is developed to utilize an automatic multi-thresholding method to handle this problem by combining the histogram analysis and the Otsu clustering. The histogram evaluations can decide the superior number of clusters firstly. The Otsu classification algorithm solves the given medical image by continuously separating the input gray-level image by multi-thresholding until reaching optimal smooth rate. The method solves exactly the problem of the uncertain contoured objects in medical image by using the Otsu clustering classification with automatic multi-thresholding operation.

KEYWORDS

Automatic multi-thresholding; histogram analysis; Otsu clustering; smooth rate; Tumor

1. Introduction

Because it is important for understanding the human body anatomy, physiological processes, function of organs, and behavior of whole or a part of a organ for an abnormal physiological conditions (Enzinger & Weiss, 1995), (Rangarajan, Hsiao, & Gindi, 2000), disease image recognition plays a key role in medical image analysis and detection assistant system (Tu et al., 2001). For the last two decades, the detailed knowledge of anatomical structures has been witnessed a revolutionary progress in medical imaging and computerized medical image processing for clinical practice, they will be helpful for diagnosis and treatment evaluation and intervention. For the computerized image classification, it is very important to identify the anatomical areas of interest for diagnosis, therefore, reconstruction, processing and analysis methods have been developed for these medical imaging applications. Because the different scanners will make available information about different tissue properties, the physician may use several scanner types for a proper assessment.

The disease-based image detection is a special category of image retrieval methods that can detect the abnormal image rather than just tissue images. In these most traditional medical image retrieval schemes, which retrieve some images, which are judged to be a tumor image according to some characteristics such as analysis approaches (Hauwe & Ramon, 2001), (Lashari & Ibrahim, 2013) explored for computer-aided diagnosis to improve the sensitivity and specificity of radiological tests involving medical images. These multidimensional digital images of physiological structures can be processed and manipulated to visualize hidden characteristic diagnostic features (Krinidis & Chatzis, 2010), (Lingras & West, 2004), (Ouyang, Wang, Johnson, Hu, & Chen, 1994), (Akgul, Kambhamettu, & Stone, 1998), (Abeyratne, Petropulu, & Reid, 1996), (Cohen, Georgiou, & Halpern, 1997), (Grewera & Udupa, 1996), (Georgiou & Cohen, 1998), (Donohue,

Forsberg, Piccoli, & Goldberg, 1999). For example, in the field of medical brain images, Clarke et al. (1995) presented the multispectral nature of the medical brain images data for breast tissue characterization. Soltanian-Zadeh & Windham (1992) proposed for the analysis of multiparameter medical brain images data, other approaches include the maximum contrast method (Soltanian-Zadeh, Windham, Peck, & Yagle, 1992), artificial neural networks (Alirezai, Jernigan, & Nihmias, 1995), (Maji & Pal, 2007), (Ozkan, Dawant, & Maciunas, 1993), (DeLa Paz, Herskovits, Gesu, Hanson, & Bernstein, 1990), (Simmons, Arridge, Barker, Cluckie, & Tofts, 1994), (Ji et al., 2012), (Brandt, Bohant, Kramer, & Fletcher, 1994), a rough set model by deciding a variety of clustering techniques (Phillips et al., 1995), (Velthuisen et al., 1995), (Vaidyanathan et al., 1995), (Soltanian-Zadeh, Windham, & Jenkins, 1990), (Peck, Windham, Soltanian-Zadeh, & Roebuck, 1992), (Soltanian-Zadeh, Windham, & Yagle, 1993), (Soltanian-Zadeh & Windham, 1994), (Soltanian-Zadeh, Windham, & Peck, 1996), based on eigenimage filtering (Peck et al., 1996), (Kurita, Otsu, & Abdelmalek, 1992), and a definition of optimal feature space method (Juang & Wu, 2010), all of them have been applied for bio-tissue classification and characterization.

Image classification methods usually are widely classified into three categories: Edge-based methods, where the edge information is used for object boundaries; Pixel-based direct classification method, where heuristics or estimation method derived from the histogram statistics of the image is used for the forming closed regions; Region-based method, where pixels are analyzed directly for a region growing process based on a pre-defined similarity principle to form closed region. In these region-based methods, clustering method is very suitable for classifying the regions as the distribution of the bio-tissues, specially for the application on medical brain images classification. The medical brain images tissue image is often divided into the white matter (WM), the gray matter (GM) and

the cerebrospinal uid (CSF). An effective separation of WM, GM and CSF is very important for the quantitative analysis, when the clustering regions are defined, these features can be extracted to represent these regions of their characterization. They include shape and texture information of the tumor regions as well as their statistical properties. In this research, we will propose a detection method by using Otsu clustering with automatic multi-thresholding setup for medical brain images tumor. The difference with the old Otsu clustering (Kurita et al., 1992) and other threshold method (Juang & Wu, 2010, authors' previous work), our proposed method develops an automatic multi-thresholding divided into the regional classifications. The research method is easy and fast to classify the tumor region comparing with other medical brain images classification methods (Juang & Wu, 2010) (authors previous work) under the same computer's tool implementation. The proposed multi-thresholding technique is now discussed as follow:

2. The Image Processing Methodology

An image process procedure to classify disease images using Otsu clustering with automatic multi-thresholding setup for medical brain images tumor was proposed in this study. To show an accurate classification, a proper image process procedure for an image can be manually selected to fit the best accuracy. But, as the number of images increase, this region selection process may become tedious. It may be a more useful tool if the system can analyze the images and locate suitable regions. Therefore, a proper image process procedure is proposed to facilitate the image classification process.

Segmentation is a major step in medical image analysis and classification for radiological evaluation or computer-aided diagnosis. Image segmentation is the process of partitioning an image into distinct region by grouping together neighborhood pixels based on some pre-defined similarity criterion. The similarity principle can be determined using specific properties or features of pixels representing objects in the image. So, segmentation is a pixel classification technique that allows the formation of regions of similarities in the image. Image segmentation methods can be widely classified into three categories: Edge-based methods, where the edge information is used for boundaries of objects. The boundaries are then analyzed and modified, if necessary, to form closed regions belonging to the objects in the image; Pixel-based direct classification method, where heuristics or estimation method derived from the histogram statistics of the image are used for forming closed regions belonging to the objects in the image; Region-based method, where pixels are analyzed directly for a region growing process based on a pre-defined similarity principle to form closed region belonging to the objects in the image. When the regions are defined, features can be computed to represent regions for characterization, analysis and classification. These features will include shape and texture information of the regions as well as statistical properties, like variance and mean of gray values. In this paper, the proposed technique consists of four major elements: Background removal process, automatic multi-thresholding setup, Otsu clustering process, and digitalization. The image process procedure for medical brain images classification is shown in Figure 1. Here S represents smooth rate. The following sections are based on Figure 1 flowchart for the relative image processing algorithm description.

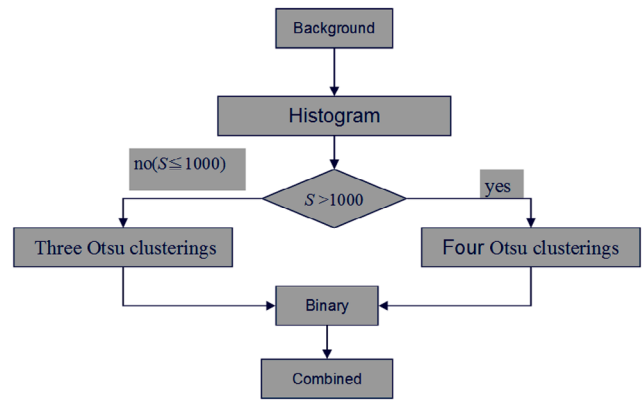


Figure 1. Flowchart for Brain Tumor Image Classification Processing.

2.1. Background Removal

Because Otsu multi-thresholding method will give the improper results when the object size is very different from background, we first use background removal process to reduce the affection on the threshold value, and then find an optimal threshold value. Because the medical brain images is a gray-scale, its background is black, which has an impact on threshold values, before we do Otsu multi-thresholding process, we take the following steps to remove all of the background factors:

- (1) Make a horizontal reconnaissance from the original brain image Figure 2(a) left and right respectively, if the adjacent pixels gap does not exceed 2 (changeable value), it is a homogeneous part (remove), and if it is above 2, it is not a homogeneous part (remain), then produce like Figure 2(b) block.
- (2) Make a vertical reconnaissance from the original brain image Figure 2(a) up and down respectively, if the adjacent pixels gap does not exceed 2 (changeable value), it is a homogeneous part (remove), and if it is above 2, it is not a homogeneous part (remain), then produce like Figure 2(c) block.
- (3) Make the intersection of Figure 2(b) and Figure 2(c) to produce like Figure 2(d). The graph appeals a lower quality for the purpose to explain background contrast.

2.2. Automatic Multi-thresholding

In this stage, we process the dark and bright brain images for tumor region using automatic multi-thresholding setup. First we acquire a histogram from the background removal image as shown in Figure 3, (the graph appeals a lower quality for the purpose to explain background contrast), moving the x axis of histogram, and then the y axis of histogram representing the pixel number will decline from the highest number (maximal point) to the lowest number (minimal point) displaying smooth status; on tumor clearer images its histogram is rapidly declining. From the declining curve, we can evaluate the smooth rate of the histogram as follows:

$$S = \frac{\sum_{i=m}^n ((i, 1) - (i + 1, 1))^2}{n - m} \quad (1)$$

where m is the maximum number of pixel value and n is the minimum number of pixel value. Because the image classification

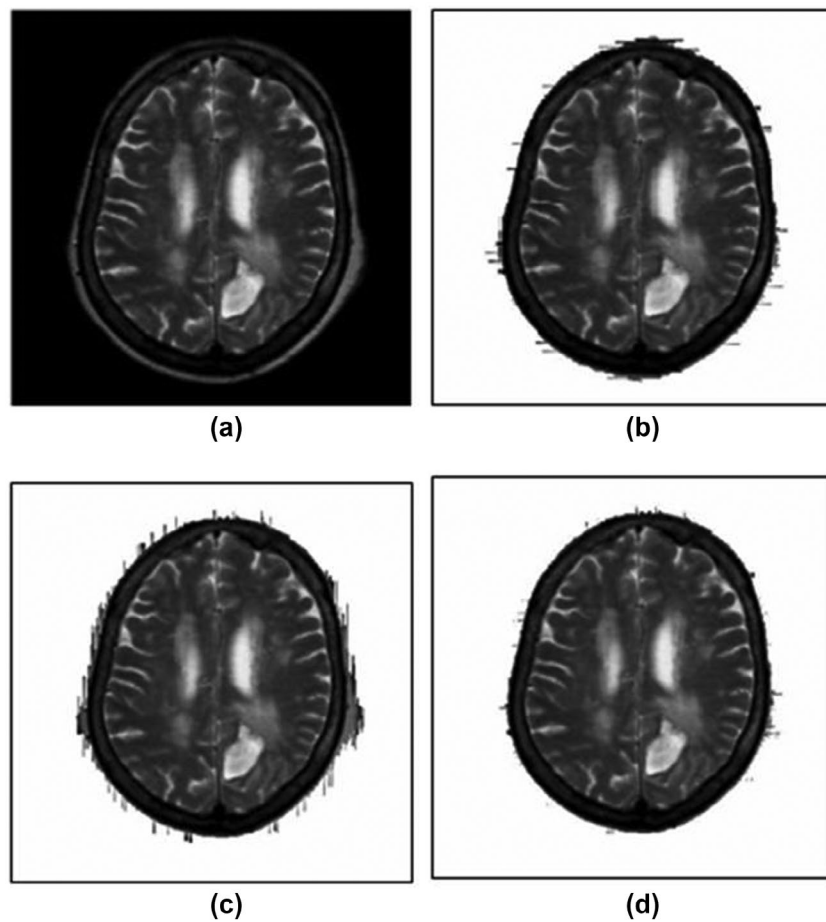


Figure 2. The Background Removal Process (a) Original Medical Brain Images (b) After Horizontal Background Removal Image (c) After Vertical Background Removal Image (d) After Composition Image.

decision is made from m to n curve smoothing, n must be greater than m . If the curve in the histogram slowly declines down from its highest point to its lowest point, it means the image is dark and its smooth rate is high, as shown in Figure 3(a). It means there is a lower contrast and the quantity of dark pixels is high. In other words, if the curve in the histogram sharply declines down from its highest point to its lowest point, it means the image is bright and its smooth rate is low, as shown in Figure 3(b). It means there is a higher contrast and the quantity of bright pixels is high. When we get a smooth rate, then the threshold value for the next stage will be determined automatically from it as shown in Figure 1. The real automatic multi-thresholding setup processes will be discussed in classification test section.

2.3. Otsu Multi-thresholding Method

The pixel value method is based on histogram statistics for defining single or multiple thresholds to classify a gray level image. We can obtain the threshold for classifying pixels into classes from the analysis of the histogram of the image and examine the histogram for the bimodal distribution. The threshold will be set into the gray value corresponding to the bottom point in the histogram valley as shown in Figure 4 when the histogram is bimodal. The image can be partitioned into two or more regions using some heuristics about the properties of the image when it is false.

The histogram of each partition is used to determine thresholds, and then pixel value can be classified into one or the two

classes by comparing the gray value of each pixel to the selected threshold. An image $f(x, y)$ classes use a gray value threshold t then

$$g(x, y) = \begin{cases} 1 & \text{if } f(x, y) > T^* \\ 0 & \text{if } f(x, y) \leq T^* \end{cases} \quad (2)$$

where $g(x, y)$ is separated gray values “1” and “0” and t is the threshold selected at the bottom point of the histogram.

We analyze the histogram for the peak values and then finding the deepest bottom point between the two consecutive major peaks to determine the gray value threshold t . We judge this method shows good results when a histogram is clearly bi-modal. However, medical images may have multiple peaks with specific requirements of regions to be classified. For instance, the medical brain images may have many major peaks in the histogram. It can be noted that there are some holes within the classified brain region using the gray value threshold. These holes can be filled out to quantify the overall brain area under the skull in the image. To classify specific brain regions like ventricles, we need additional thresholds determined from the histogram. These thresholds will be determined by finding additional peaks in the histogram remaining distribution belonging to the second major peak. Usually, these thresholds will be determined from the peaks and analysis of the remaining histograms in a recursive manner. So, the Otsu multi-thresholding method is adopted for the brain image classification.

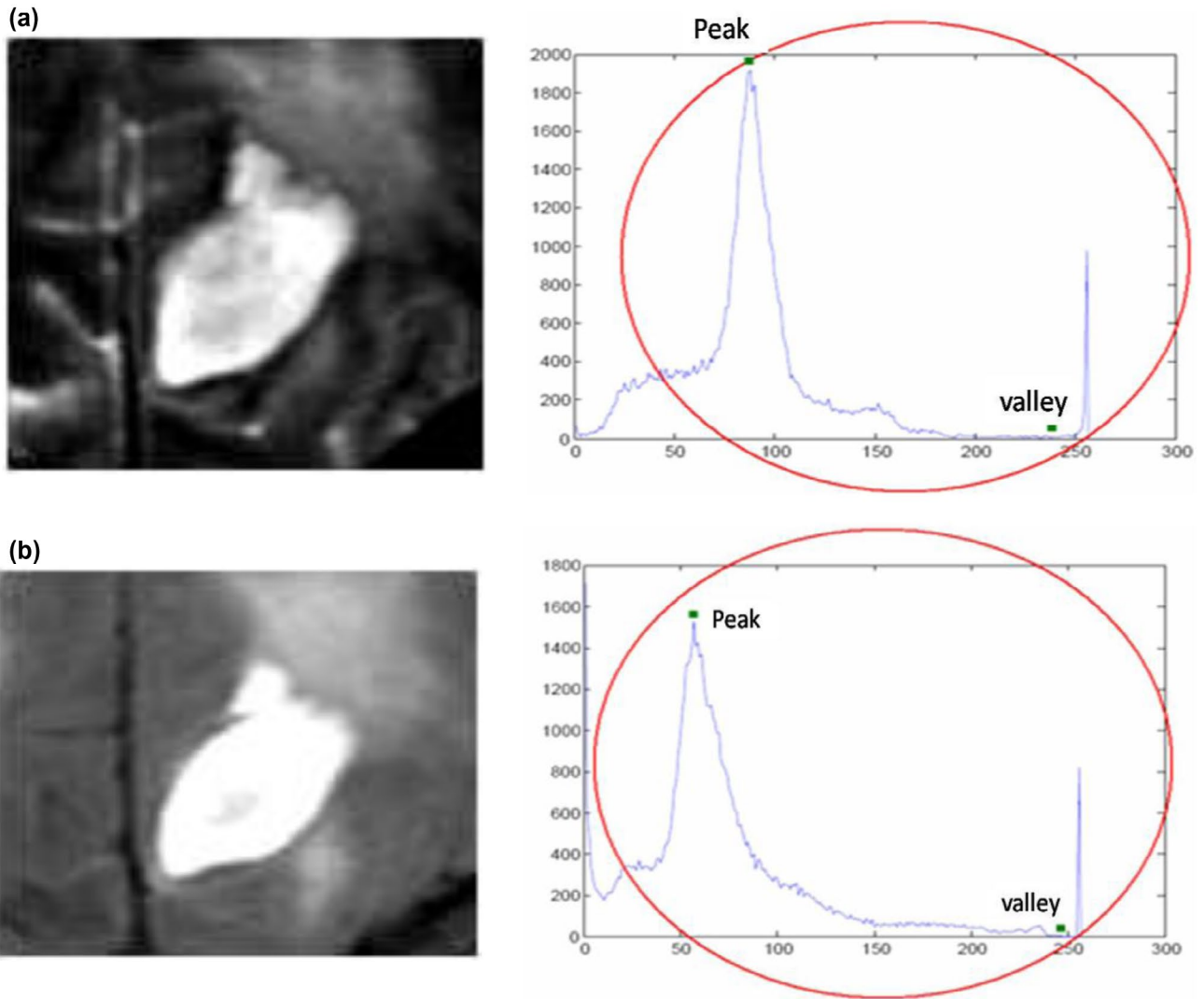


Figure 3. The Smooth Rate Process from (a) a Dark Brain Image (Higher Smooth Rate) and (b) a Bright Brain Image (Lower Smooth Rate).

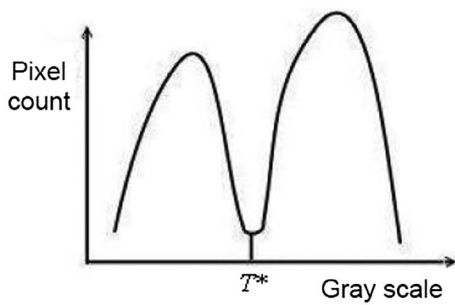


Figure 4. The Multi-thresholding Process Example based on Histogram Statistics, T^* is an Optimal Threshold Value.

Now suppose that the pixels are partitioned into two classes C_0 and C_1 (background and objects) by a threshold T^* , then the *weighted within-class variance* is given by

$$\sigma_w^2(t) = q_1(t)\sigma_1^2(t) + q_2(t)\sigma_2^2(t) \quad (3)$$

where the class probabilities are estimated as

$$q_1(t) = \sum_{i=1}^t P(i) \quad (4)$$

$$q_2(t) = \sum_{i=t+1}^I P(i) \quad (5)$$

and the class means are given by

$$\mu_1(t) = \frac{\sum_{i=1}^t iP(i)}{q_1(t)} \quad (6)$$

$$\mu_2(t) = \frac{\sum_{i=t+1}^I iP(i)}{q_2(t)}. \quad (7)$$

Finally, the individual class variances

$$\sigma_1^2(t) = \frac{\sum_{i=1}^t [i - \mu_1(t)]^2 P(i)}{q_1(t)} \quad (8)$$

$$\sigma_2^2(t) = \frac{\sum_{i=t+1}^I [i - \mu_2(t)]^2 P(i)}{q_2(t)} \quad (9).$$

Next, all we need to do is just run through the full range of t values and pick the value that minimizes, but the relationship between the within-class and between-class variances can be exploited to generate a recursion relation that permits a much faster calculation. The basic idea is that the total variance does not depend on threshold (obviously). For any given threshold, the total variance is the sum of the within-class variances

(weighted) and the between class variance, which is the sum of weighted squared distances between the class means and the grand mean. After some algebra, we can express the total variance as:

$$\sigma^2 = \sigma_w^2(t) + q_1(t)[1 - q_1(t)][\mu_1(t) - \mu_2(t)]^2 \quad (10)$$

the between-class variance matrix is defined as

$$\sigma_b^2(t) = q_1(t)[1 - q_1(t)][\mu_1(t) - \mu_2(t)]^2 \quad (11)$$

Since the total is constant and independent of T^* , the effect of changing the threshold is merely to move the contributions of the two terms back and forth. The nice thing about this is that we can compute the quantities in $\sigma_b^2(t)$ recursively as we run through the range of t values.

Finally, we initialize $q_1(1) = P(1)$, $\mu_1(0) = 0$, then we use the following fast recursive algorithm to realize the above method;

$$q_1(t + 1) = q_1(t) + P(t + 1) \quad (12)$$

$$\mu_1(t + 1) = \frac{q_1(t)\mu_1(t) + (t + 1)P(t + 1)}{q_1(t + 1)} \quad (13)$$

$$\mu_2(t + 1) = \frac{\mu - q_1(t + 1)\mu_1(t + 1)}{1 - q_1(t + 1)} \quad (14)$$

Multi-thresholding is for the process of grouping data points with similar feature vectors together in a single cluster while data points with dissimilar feature vectors are placed in different clusters. Therefore the data points that are close to each other in the feature space are clustered together. The similarity of feature vectors can be represented by an appropriate distance measure such as Euclidean or Mahalanobis distance. Each cluster is represented by its mean (centroid) and variance (spread) associated with the distribution of the corresponding feature vectors of the data points in the cluster. The formation of clusters is optimized with respect to an objective function involving pre-specified distance and similarity measures along with additional constraints like smoothness. So, we propose the automatic multi-thresholding value grouping based smooth rate added into Otsu clustering process to obtain better results. The process steps as shown in Figure 5 are as follows:

- (1) First use Otsu multi-thresholding algorithm to get a threshold value, and then divide it into two groups of (C1, C2).
- (2) Second use Otsu multi-thresholding algorithm on C1 and C2 again for further processing to divide C1 into two groups of (C1a, C1b), and C2 into two groups of (C2a, C2b).
- (3) Third continuously use Otsu multi-thresholding algorithm on C1a, C1b, C2a, and C2b for further processing to divide them into C1a+, C1a-, C1b+, C1b-, C2a+, C2a-, C2b+, and C2b-.

How many groups to separate is depended on the original image threshold value. The automatic multi-thresholding setup processes is based on the gray-level image 0–255 for classification, after this processes, the processed image is still a gray-level image, therefore it can be for binary processes. The real Otsu multi-thresholding processes will be discussed in classification test section.

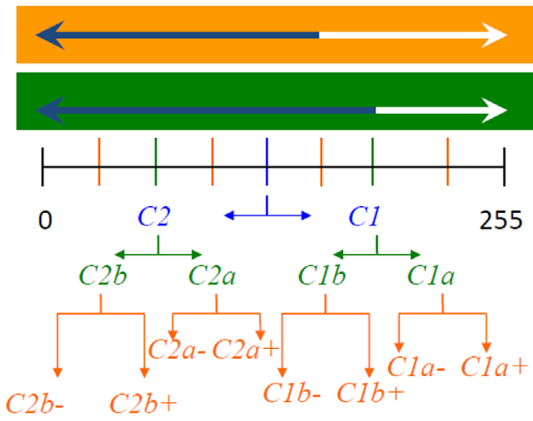


Figure 5. The Grouping Explanation for the Automatic Multi-thresholding Value Grouping by Adding Smooth Rate into Otsu Clustering Process.

Table 1. Calculation for smooth rate and threshold number.

Figure no.	Smooth rate	Threshold number
Figure 6	622.6061	3
Figure 7	845.1294	3
Figure 8	600.3182	3
Figure 9	1,446.1986	4
Figure 10	2,025.6033	4
Figure 11	1866.0323	4
Figure 12	1,324.1310	4
Figure 13	1,353.3969	4
Figure 14	1,544.6194	4

2.4. Digitalization

Digitalization process was used to form the object contour after Otsu multi-thresholding process. A digitalization image only has black and white. A gray-level image can become a binary image using choosing a gray-level t from the original image, then change every pixel into black or white based on its gray value greater than or less than t as follows:

A pixel turns

$$\begin{cases} \text{white} & \text{if } x > t \\ \text{black} & \text{if } x \leq t \end{cases} \quad (15)$$

where x is gray value.

The real digitalization processes will be discussed in classification test section.

3. Test and Analysis

These medical images may also require classification using a multi-dimensional feature space with multiple parameters of interest. Images can be classified by pixel classification through multi-thresholding of all features of interest. The number of clusters in the multi-dimensional feature space thus represents the number of classes in the image. As the image is classified into cluster classes, classified regions are obtained by checking the neighborhood pixels for the same class label. However, multi-thresholding may produce disjoint regions with holes or regions with a single pixel. After the image data are clustered and pixels are classified, a post-processing algorithm such as region growing, pixel connectivity or rule-based algorithm is usually applied to obtain the final classified regions.

The following tests show how to use Otsu clustering with automatic multi-thresholding setup technique to track a tumor from a medical brain image (288×288), which is stained with tumor as shown in Figure 2(a). First, we do background removal from the original image. Then, we must calculate the smooth

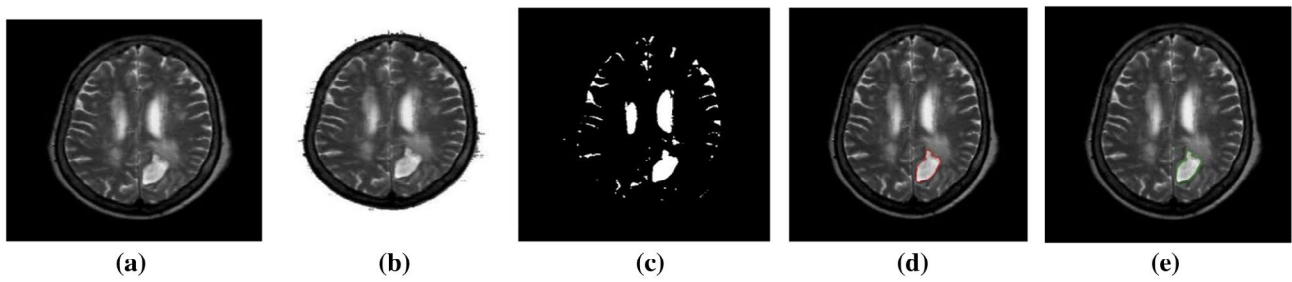


Figure 6. (a) Is the First-case for the Original Medical Brain Images T1 Image, (b) is for After Background Removal Image, (c) is for After Binary Image, (d) is for After Classification Image, and (e) is for Hand Drawing Image.

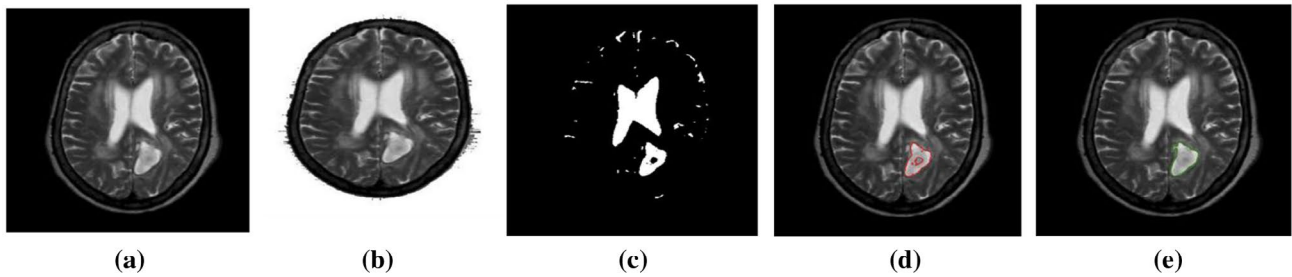


Figure 7. (a) Is the Second-case for the Original Medical Brain Images T1 Image, (b) is for After Background Removal Image, (c) is for After Binary Image, (d) is for After Classification Image, and (e) is for Hand Drawing Image.

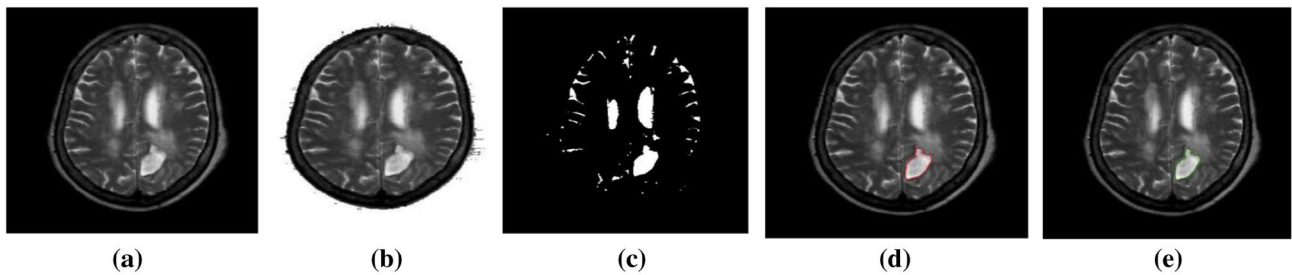


Figure 8. (a) Is the Third-case for the Original Medical Brain Images T1 Image, (b) is for After Background Removal Image, (c) is for After Binary Image, (d) is for After Classification Image, and (e) is for Hand Drawing Image.

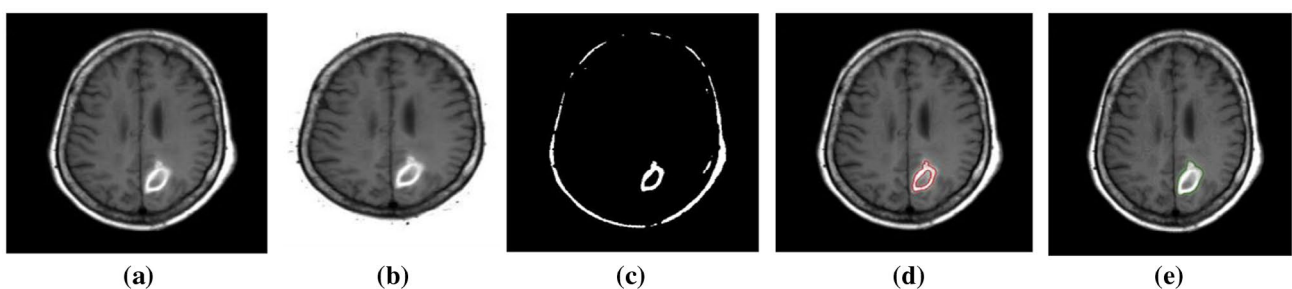


Figure 9. (a) Is the First-case for the Original Medical Brain Images T2 Image, (b) is for After Background Removal Image, (c) is for After Binary Image, (d) is for After Classification Image, and (e) is for Hand Drawing Image.

rates of these brain images according to equation (1) to decide their thresholding setup number, that is, Otsu multi-thresholding grouping number. The results are shown in Table 1. The switch smooth rate is 1,000 according to the thirty-two medical brain images histogram statistic analysis. When the smooth rate is above 1,000, the Otsu multi-thresholding grouping number is 4. When the smooth rate is below 1,000, the Otsu multi-thresholding grouping number is 3. According to the experiment test, three or four times of Otsu multi-thresholding grouping is the optimal grouping for the brain image classification as shown in Figure 1. Otsu multi-thresholding treats each

object as having a location in space. It finds partitions such that objects within each cluster are as close to each other as possible, and as far from objects in other clusters as possible. Otsu multi-thresholding requires specifying the number of clusters to be partitioned and a distance metric to quantify how close two objects are to each other. After Otsu multi-thresholding processing, then binarize the brain image to form the tumor region contour and combine it with the original image, finally the tumor classification comes out. In this paper, we test three different kinds of medical brain images modalities (T1, T2, and spin density) with a total of nine images, which will be enough

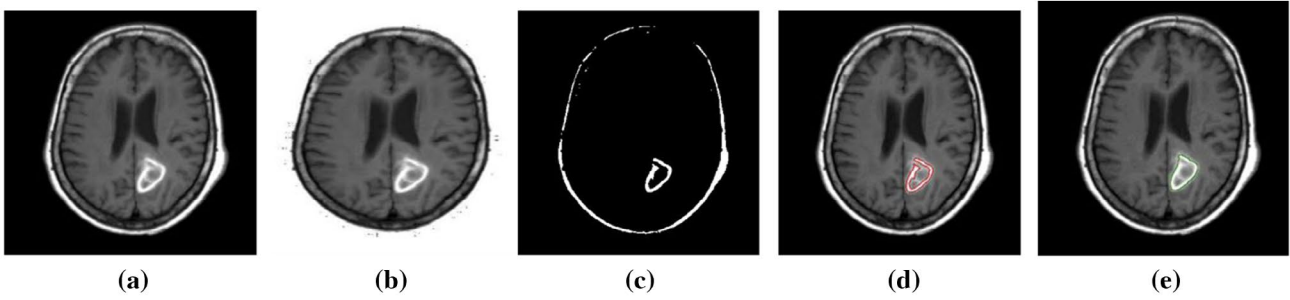


Figure 10. (a) Is the Second-case for the Original Medical Brain Images T2 Image, (b) is for After Background Removal Image, (c) is for After Binary Image, (d) is for After Classification Image, and (e) is for Hand Drawing Image.

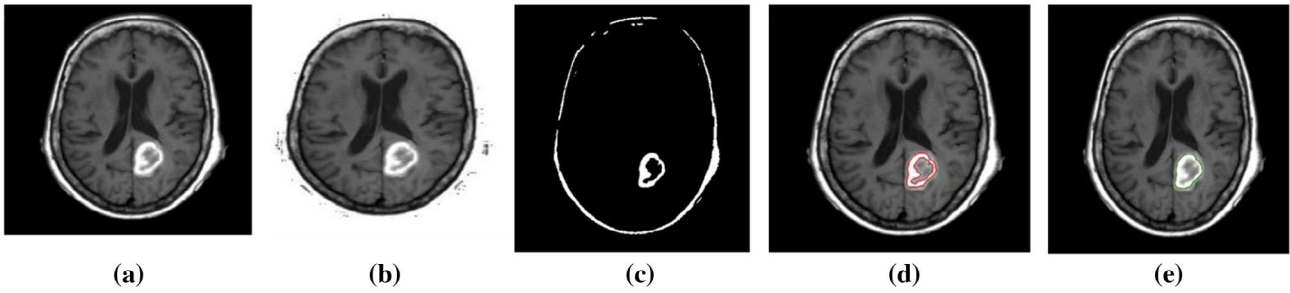


Figure 11. (a) Is the Third-case for the Original Medical Brain Images T2 Image, (b) is for After Background Removal Image, (c) is for After Binary Image, (d) is for After Classification Image, and (e) is for Hand Drawing Image.

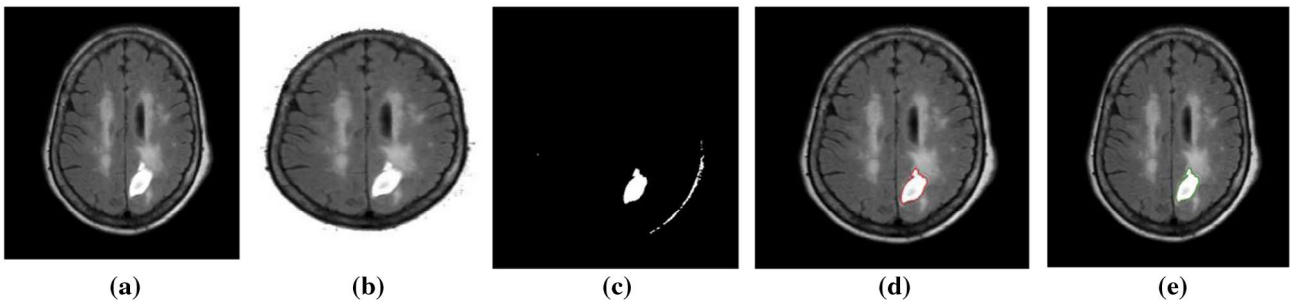


Figure 12. (a) Is the First-case for the Original Medical Brain Images Spin-density Image, (b) is for After Background Removal Image, (c) is for After Binary Image, (d) is for After Classification Image, and (e) is for Hand Drawing Image.

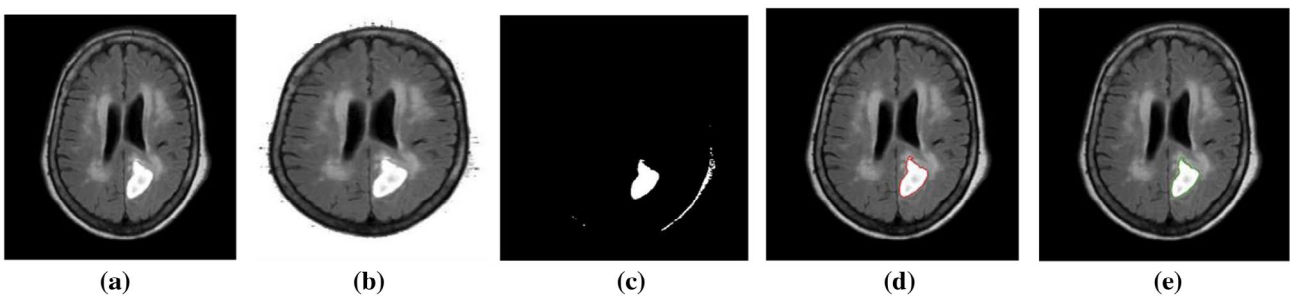


Figure 13. (a) Is the Second-case for the Original Medical Brain Images Spin-density Image, (b) is for After Background Removal Image, (c) is for After Binary Image, (d) is for After Classification Image, and (e) is for Hand Drawing Image.

for checking the proposed method accuracy. Usually, medical brain images can take lots of images, but only has three type images to represent the different medical brain images modalities. Figure 6(a) is the first-case for the original medical brain images T1 image, Figure 6(b) is for after background removal image, Figure 6(c) is for after binary image, Figure 6(d) is for after classification image, and Figure 6(e) is for hand drawing image, Figure 7(a)-(e) are the second-case images and Figure

8(a)-(e) are the third-case images. Figure 9(a)-(e) are the first-case for the original medical brain images T2 image, Figure 10(a)-(e) are the second-case images and Figure 11(a)-(e) are the third-case images. Figure 12(a)-(e) are the first-case for the original medical brain images spin-density image, Figure 13(a)-(e) are the second-case images and Figure 14(a)-(e) are the third-case images. To compute the brain tumor classification accuracy, we need to make the tumor region contour by a

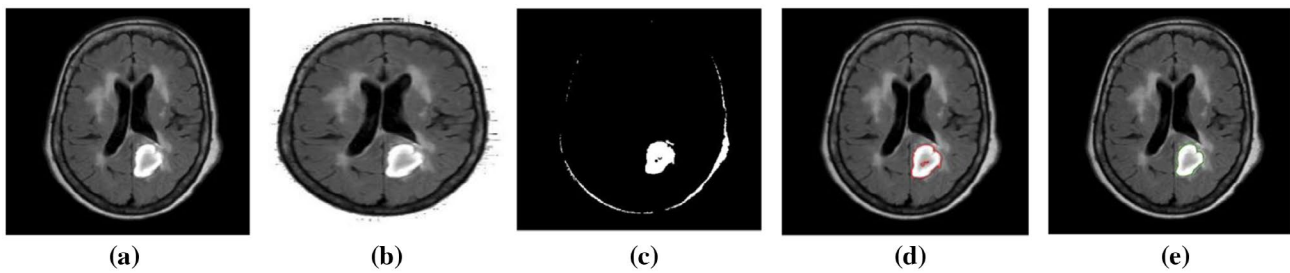


Figure 14. (a) Is the Third-case for the Original Medical Brain Images Spin-density Image, (b) is for After Background Removal Image, (c) is for After Binary Image, (d) is for After Classification Image, and (e) is for Hand Drawing Image.

Table 2. Accuracy for Otsu multi-thresholding classification processing.

Figure no.	Accuracy (%)
Figure 6	96.23%
Figure 7	96.49%
Figure 8	96.22%
Figure 9	97.53%
Figure 10	97.69%
Figure 11	97.54%
Figure 12	98.78%
Figure 13	98.30%
Figure 14	98.36%

Table 3. Time complexity for Otsu multi-thresholding classification processing steps.

Step	Backgroundremoval	Threshold setup	Otsu multi-thresholding	Binary image
Time complexity (O)	N	N	N	N

hand drawing as shown in Figure 6(e)-Figure 14(e), which are assumed 100% accuracy, the results are shown in Table 2. In general, the average accuracy is good above 90%. The experimental results demonstrate that the misclassification error is very small between the proposed result and hand drawing. Therefore the research method has an excellent accuracy and it is much suitable for any kind of medical brain images modality. Their time complexities for the proposed method processing step is shown in Table 3. The results show the research procedure has a normal time complexity (O). N is lower time complexity and N^2 is normal time complexity. Comparing with other medical brain images classification methods (Juang & Wu, 2010) (authors previous work) under the same computer's tool implementation, the research method has much lower time complexity, which means lots saving computing time and less process procedure. In addition, its accuracy is much higher than them (Juang & Wu, 2010) (authors previous work) under the same computer's tool implementation.

Finally, the experiment tests shows that the proposed method can categorize thresholding setup number and classification effectively the tumor location and size regardless of the original image's brightness and structure.

4. Conclusions

A tumor detection method of medical brain images using Otsu clustering with automatic multi-thresholding setup technique has been developed. The analysis result of medical brain images shows significant breakthrough. The multi-thresholding classification algorithm for detection objects in medical images is performed to be very helpful for medical brain images applications. The brain regions related to a tumor can be precously

extracted from the original brain image. It will be able to help pathologists for further surgery and medicine treatment.

Acknowledgement

The authors deeply acknowledge the financial support from Xiamen University of Technology, Fujian, P.R. China under the Xiamen University of Technology Scientific Research Foundation for Talents plan.

Disclosure statement

No potential conflict of interest was reported by the authors.

Notes on contributors



Li-Hong Juang received a B.S. degree in Civil Engineering from the National Chiao Tung University, Taiwan in 1990, and M. S. degree in Applied Mechanics from the National Taiwan University, Taiwan in 1993, and a Ph.D. degree in Control and Embedded System Group from the Department of Engineering at Leicester University, UK, in 2006. Now he is a Professor at School of Electrical Engineering and Automation, Xiamen University of Technology, P. R. China. His research interests are in the analysis, modeling, smart system design, image process, machine vision, robot control and medical system.



Ming-Ni Wu received a Ph.D. degree in Computer Science & Information Engineering, National Chung Cheng University, Taiwan. She is now an associate professor in the Department of Information Management, National Taichung University of Technology, Taiwan ROC. Her research interests are in image process and information management.

References

- Abeyratne, U.R., Petropulu, A.P., & Reid, J.M. (1996). On modeling the tissue response from ultrasonic B-scan images. *IEEE Transactions on Medical Imaging*, 15, 479–490.
- Akgul, Y.S., Kambhamettu, C., & Stone, M. (1998). Extraction and tracking of the tongue surface from ultrasound image sequences. In Proceedings IEEE computer vision pattern recognition. Santa Barbara, CA, 298–303.
- Alirezai, J., Jernigan, M.E., & Nihmias, C. (1995). Neural network based segmentation of magnetic resonance images of the brain. *Proc IEEE Conf Med Imag*, 1397–1401.
- Brandt, M.E., Bohant, T.P., Kramer, L.A., & Fletcher, J.M. (1994). Estimation of CSE, white and gray matter volumes in hydrocephalic children using fuzzy clustering of MR images. *Journal of the Computerized Medical Imaging Society*, 18, 25–34.
- Clarke, L.P., Velthuizen, R.P., Camacho, M.A., Heine, J.J., Vaidyanathan, M., Hall, L.O., ... Silbiger, M.L. (1995). MRI segmentation: Methods and applications. *Magnetic Resonance Imaging*, 13, 343–368.
- Cohen, F.S., Georgiou, G., & Halpern, E. (1997). WOLD decomposition of the backscatter echo in ultrasound images of soft tissue organs. *IEEE Transactions on Ultrasonics, Ferroelectrics and Frequency Control*, 44, 460–472.

- DeLa Paz, R.L., Herskovits, E.H., Gesu, V. Di, Hanson, W.A., & Bernstein, R. (1990). Cluster analysis of medical magnetic resonance images (MRI) data: Diagnostic application and evaluation. *J. SPIE*, 1259, 176–181.
- Donohue, K.D., Forsberg, F., Piccoli, C.W., & Goldberg, B.B. (1999). Classification of breast masses with ultrasonic scattering structure templates. *IEEE Transactions on Ultrasonics, Ferroelectrics and Frequency Control*, 46, 300–310.
- Enzinger, F.M., & Weiss, S.W. (1995). Malignant vascular tumors. In F.M. Enzinger, S.W. Weiss, (Eds.), *Soft tissue tumors* (pp. 655–677). 3rd ed. St Louis, MO: Mosby.
- Georgiou, G., & Cohen, F.S. (1998). Statistical characterization of diffuse scattering in ultrasound images. *IEEE Transactions on Ultrasonics, Ferroelectrics and Frequency Control*, 45, 57–64.
- Grewera, G.J., & Udupa, J.K. (1996). Shape based interpolation of multidimensional grey-level images. *IEEE Transactions on Medical Imaging*, 15, 881–892.
- Hauwe, L.V.D., & Ramon, F. (2001). Lymphatic tumors. In A.M. De Schepper (Ed.), *Imaging of soft tumors*, 2nd ed., (pp. 246–254). Heidelberg: Springer.
- Ji, Z., Sun, Q., Xia, Y., Chen, Q., Xia, D., & Feng, D. (2012). Generalized rough fuzzy c-means algorithm for brain MR image segmentation. *Computer Methods and Programs in Biomedicine*, 108, 644–655.
- Juang, L.H., & Wu, M.N. (2010). MRI brain lesion image detection based on color-converted K-means clustering segmentation. *Measurement*, 43, 941–949.
- Krinidis S., & Chatzis V. (2010). A robust fuzzy local information c- means clustering algorithm. *IEEE Transactions on Image Processing*, 19, 1328–1337.
- Kurita, T., Otsu, N., & Abdelmalek, N. (1992). Maximum Likelihood Thresholding Based on Population Mixture Models. *Pattern Recognition*, 25, 1231–1240.
- Lashari, S.A., & Ibrahim, R. (2013). A framework for medical images classification using soft set. *Procedia Technology*, 11, 548–556.
- Lingras P., & West C. (2004). Interval set clustering of web users with rough k-means. *Journal of Intelligent Information Systems*, 23, 5–16.
- Maji, P., & Pal, S.K. (2007). Rough set based generalized fuzzy c-means algorithm and quantitative indices. *IEEE Transactions on Systems, Man, and Cybernetics, Part B (Cybernetics)*, 37, 1529–1540.
- Ouyang, X., Wang, W.H., Johnson, V.E., Hu, X., & Chen, C.T. (1994). Incorporation of correlated structural images in PET image reconstruction. *IEEE Transactions on Medical Imaging*, 13, 627–640.
- Ozkan, M., Dawant, B.M., & Maciunas, R.J. (1993). Neural-network-based segmentation of multi-modal medical images: A comparative and prospective study. *IEEE Transactions on Medical Imaging*, 12, 534–544.
- Peck, D.J., Windham, J.P., Emery L., Soltanian-Zadeh, H., Hearshen, D.O., & Mikkelsen, T. (1996). Cerebral tumor volume calculations using planimetric and eigenimage analysis. *Medical Physics*, 23, 2035–2042.
- Peck, D.J., Windham, J.P., Soltanian-Zadeh, H., & Roebuck, J.P. (1992). A fast and accurate algorithm for volume determination in MRI. *Medical Physics*, 19, 599–605.
- Phillips, W.E., Velthuizen, R.P., Phuphanich, S.L., Hall, O., Clarke, L.P., & Silbiger, M.L. (1995). Application of fuzzy C-means segmentation technique for tissue differentiation in magnetic resonance images of a hemorrhagic glioblastoma multiforme. *Magnetic Resonance Imaging*, 13, 277–290.
- Rangarajan, A., Hsiao, I.T., & Gindi, G. (2000). A Bayesian joint mixture framework for the integration of anatomical in functional image reconstruction. *Journal of Mathematical Imaging and Vision*, 12, 199–217.
- Simmons, A., Arridge, S.R., Barker, G.J., Cluckie, A.J., & Tofts, P.S. (1994). Improvements to the quality of MRI cluster analysis. *Magnetic Resonance Imaging*, 12, 1191–1204.
- Soltanian-Zadeh, H., Windham, J.P., & Peck, D.J. (1996). Optimal linear transformation for MRI feature extraction. *IEEE Transactions on Medical Imaging*, 15, 749–767.
- Soltanian-Zadeh, H., & Windham, J.P. (1994). Letter to the Editor: Mathematical Basis of Eigenimage Filtering. *Magnetic Resonance in Medicine*, 31, 465–466.
- Soltanian-Zadeh, H., Windham, J.P., & Yagle, A.E. (1993). Optimal transformation for correcting partial volume averaging effects in magnetic resonance imaging. *IEEE Transactions on Nuclear Science*, 40, 1204–1212.
- Soltanian-Zadeh, H., & Windham, J.P. (1992). Novel and General Approach to Linear Filter Design for CNR Enhancement of MR Images with Multiple Interfering Features in the Scene. *Journal of Electronic Imaging*, 1, 171–182.
- Soltanian-Zadeh, H., Windham, J.P., Peck, D.J., & Yagle, A.E. (1992). A comparative analysis of several transformations for enhancement and segmentation of magnetic resonance image scene sequences. *IEEE Transactions on Medical Imaging*, 11, 302–318.
- Soltanian-Zadeh, H., Windham, J.P., & Jenkins, J.M. (1990). Error propagation in Eigen image Filtering. *IEEE Transactions on Medical Imaging*, 9, 405–420.
- Tu, K.Y., Chen, T.B., Lu, H.H.S., Liu, R.S., Chen, K.L., Chen, C.M., & Chen, J.C. (2001). Empirical studies of cross-reference maximum likelihood estimate reconstruction for positron emission tomography. *Biomedical Engineering: Applications, Basis and Communications*, 13, 1–7.
- Vaidyanathan, M., Clarke, L.P., Velthuizen, R.P., Phuphanich, S., Bensaïd, A.M., Hall, L.O., Bezdek, J.C., & Silbiger, M. (1995). Comparison of supervised MRI segmentation methods for tumor volume determination during therapy. *Magnetic Resonance Imaging*, 13, 719–728.
- Velthuizen, R.P., Clarke, L.P., Phuphanich, S., Hall, L.O., Bensaïd, A.M., Arrington, J.A., Greenberg, H.M., & Silbiger, M.L. (1995). Unsupervised Tumor Volume Measurement Using Magnetic Resonance Brain Images. *Journal of Magnetic Resonance Imaging*, 5, 594–605.

